# Mechanisms by Which the Atmosphere Adjusts to an Extremely Large Explosive Event

 [1]

By
Jonathan Vigh

For
Dr. Richard Johnson

December 10, 2001

In partial fulfillment
to the requirements of
AT 735

Department of Atmospheric Science
Colorado State University

[1] Photo showing Ivy King test (500 kt yield), Enewetak Atoll, Nov. 15, 1952. Taken from 'Gallery of U.S. Nuclear Tests' web page: http://fas.org/nuke/hew/Usa/Tests/Ivy.html.

## 1. Introduction

Extremely large explosive events, defined for the purposes of this paper as the impulsive release of at least 4.18 x $10^{15}$ J or one mega-ton TNT energy equivalent in a time span of less than a minute, are rare events, especially in the atmosphere. The only natural sources for such explosions are large, violent volcanic explosions and comet/asteroid impacts. As noted by Reed (1987), only a few such events have been recorded in the past two centuries (Krakatoa Eruption, 100-150 Mt yield, 1883; Great Tunguska Comet, tens of Mt, 1908; Mt. St. Helens Eruption, few Mt, 1980). The birth of the atomic age made such events commonplace from 1952 to 1962 (Simon and Robinson, 1997) as various countries built and tested nuclear weapons with yields ranging from a few hundred tons of TNT energy equivalent to the 57 Mt device tested by the U.S.S.R in 1962. Such events cause great departure from the atmosphere's 'normal' state, so it is of great interest to ask how the atmosphere returns to a balanced state following the impulsive release of such a large amount of energy in such a small volume, on the order of a cubic kilometer for volcanic eruptions and a cubic meter for nuclear explosions.

This paper investigates four processes by which the atmosphere adjusts back to a post-blast state indistinguishable from the pre-blast state. These include an initial radiative expansion phase, a hydrodynamic expansion phase, hydrostatic and geostrophic adjustment, and ultimately diffusion, mixing, and decay to heat over the global atmosphere. Since so much data are available for the nuclear tests, I have focused on the adjustment processes that occur for low altitude nuclear air bursts with yields on the order of one Mt TNT energy equivalent. Issues related to the radioactive fallout and subsequent dispersion are ignored, as have been the chemical and climatic impacts on the atmosphere

and biosphere. The effects of ground shock, electro-magnetic pulse, and fluorescence phenomena are also ignored.

**2. Radiative Expansion**

We start our discussion[2] just after the device has exploded and experienced tens of generations of nuclear fission and fusion. Very high energy alpha and beta particles are emitted along with high energy neutrons and gamma rays. Within a millionth of a second, pressures of millions of atmospheres and temperatures of tens of millions of Kelvins develop and vaporize the device and all matter within a few meters, converting about 85% of the initial energy into kinetic energy (the remaining 15% remains as unstable radioactive nucleotides which decay from minutes to thousands of years after the explosion and will not be considered in this discussion.

Within a microsecond, most of the kinetic energy of the weapons residues is radiated as soft x-rays. These initial photons are of very high energy and are not easily absorbed in air; their mean free path is on the order of a few meters, so the energy rapidly disperses outwards in all directions by a radiative cascade of emission to the air just outside the 'fireball'. As the energy spreads over larger volumes of air, the temperature of the fireball rapidly cools to hundreds of thousands of Kelvins, and the mean free path of the photons shortens, slowing the rate of increase in size down from tens of kilometers per second to thousands of meters per second. After 0.7 milliseconds, the fireball of a one Mt blast is approximately 440 feet in diameter. When the temperature within the fireball has cooled to 300,000 Kelvins, the rate of increase in size is on the order of the local

[2] Most of the discussion of the radiative and hydrodynamic expansion phases here presented are summarized from chapters 1-3 of 'The Effects of Nuclear Weapons', by Glasstone and Dolan (1977).

acoustic velocity within the fireball (thousands of meters per second) and the radiative expansion phase comes to an end as hydrodynamic expansion begins to dominate. Figure 1 is a photo that shows the fireball just before hydrodynamic separation.

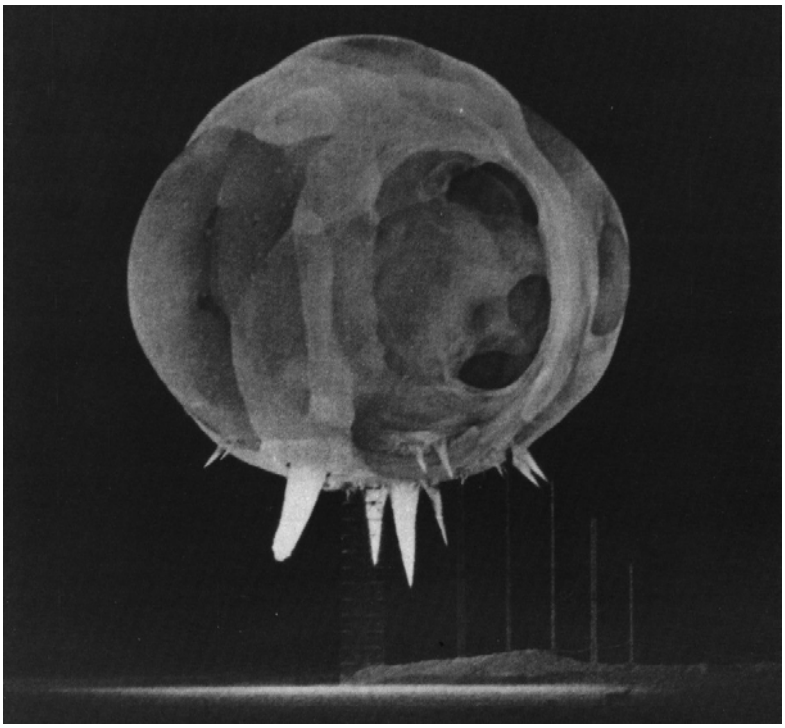

Fig. 1. Photo of one of the Snapper tests, Nevada, 1952. The early fireball is seen one millisecond after detonation and just before hydrodynamic separation occurs. The mottled appearance is due to weapons debris catching up to and splashing against the fireball front which is rapidly expanding by radiative means at this stage. The spikes protruding from the bottom are small shocks produced by the vaporization of cables/ropes that were used to stabilize the tower. Immediately after detonation, air is not a good absorber of the high energy radiation, but some objects readily absorb this radiation and are vaporized, leading to an early shock wave. Taken from 'Gallery of U.S. Nuclear Tests' web page: http://fas.org/nuke/hew/Usa/Tests/Tumblers.html

## 3. Hydrodynamic Expansion

Once the local acoustic velocity of the fireball surface exceeds the speed at which radiative expansion is occurring, a discontinuous shock travels out ahead[3], governed by

[3] As a historical note, the theoretical details of the shock produced by a point source explosion were worked out in 1941 by Sir Geoffrey Taylor and John von Neumann. Taylor's results were later declassified and published in 1950 (Taylor, 1950a). He wrote a second paper in which he made an accurate estimate of the yield of the Trinity test, even though the results were still classified (Taylor, 1950b). von Neumann's results were published as ch. 2 of a technical book in 1947 (von Neumann, 1947)

the laws of hydrodynamics. Pressure and temperature profiles at various stages of the fireball development are given in Figure 2. As the shock front passes by a point, its

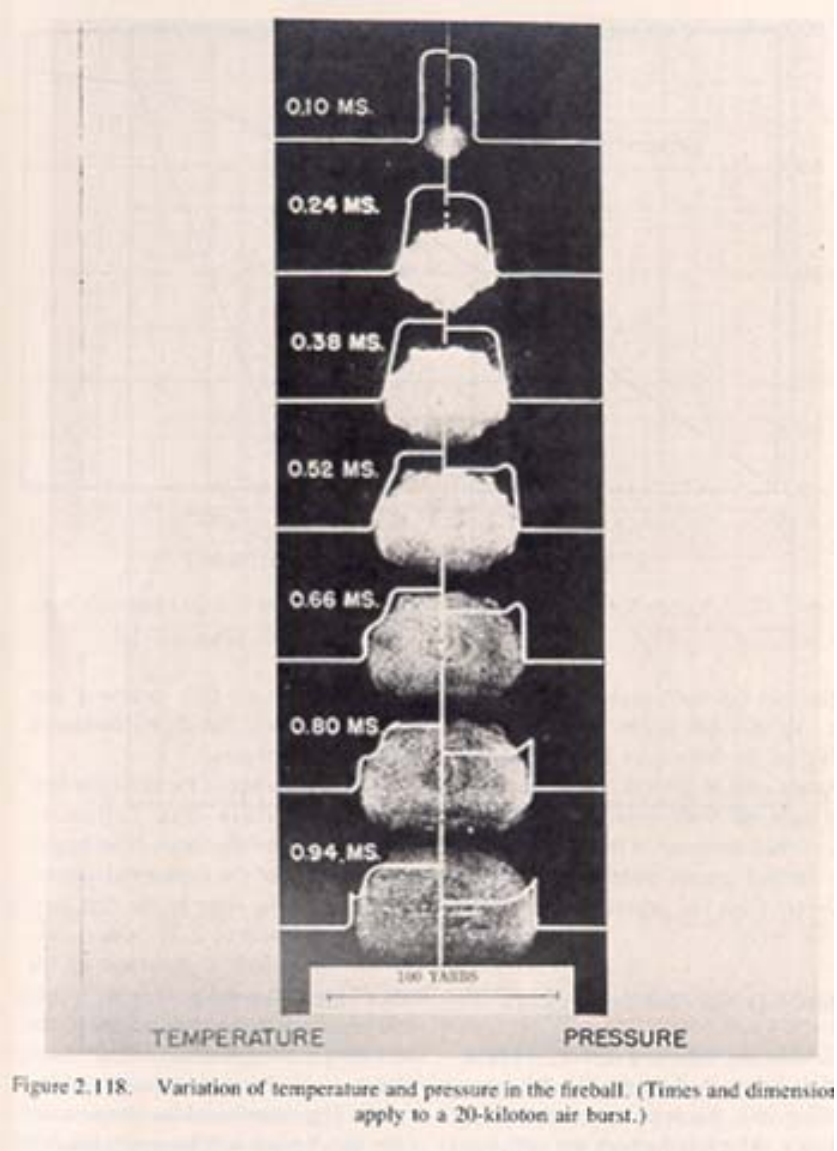


Figure 2.118. Variation of temperature and pressure in the fireball. (Times and dimensio apply to a 20-kiloton air burst.)

Fig. 2. Temperature and pressure profiles at various stages of the fireball for a 20 kt air burst. For a Mt scale burst, the appearance would be similar but the distances and times would be greater than indicated. Taken from Glasstone and Dolan, p. 67.

pressure, temperature, and density change discontinuously, but its motion does not. The violently compressed air just behind the shock front glows incandescent and radiates energy outward to the surroundings. During the period that the temperature of the shocked air is above 3000 Kelvins, it is opaque to the much more intense radiation

coming from within, so it still gains energy from within faster than is lost outward. This energy spreads over ever increasing volumes of air however, so the shock decays in strength. Once the shocked air cools below 3000 Kelvins, the fireball has reached its maximum extent, about 5700 feet in diameter for a one Mt blast, and the now invisible shock continues outwards reaching a radius of one mile in 1.4 seconds and two miles after 4.5 seconds. The cooler, transparent shock front unmasks the very hot region within, allowing a second pulse of thermal energy to be radiated to the surrounding environment. The observed vs. actual temperature of the fireball surface is given in Figure 3.

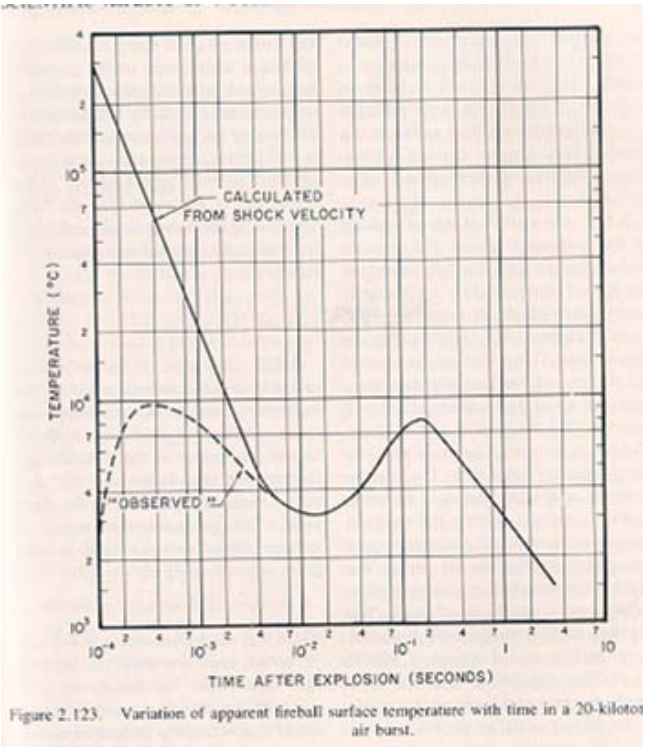

Figure 2.123. Variation of apparent fireball surface temperature with time in a 20-kiloton air burst.

Figure 3. Variation of apparent fireball surface temperature with time for a 20 kt air burst. The results for a one Mt burst are similar but take place at later times. From Glasstone and Dolan, p. 69.

All in all, about half of the initial kinetic energy escapes the immediate explosion region to the surroundings and half is dispersed by the shock front that we will now call the blast

wave, a singular pressure wave traveling at close to the local acoustic velocity within the shocked air: $U = \sqrt{RT}$ , where R is the gas constant for air and T is the local temperature.

As the blast wave travels outward, it does work compressing the ambient air and its peak 'overpressure', that is the pressure in excess of the ambient pressure, steadily decreases. The profile of the pressure wave and change in time is given in Figure 4.

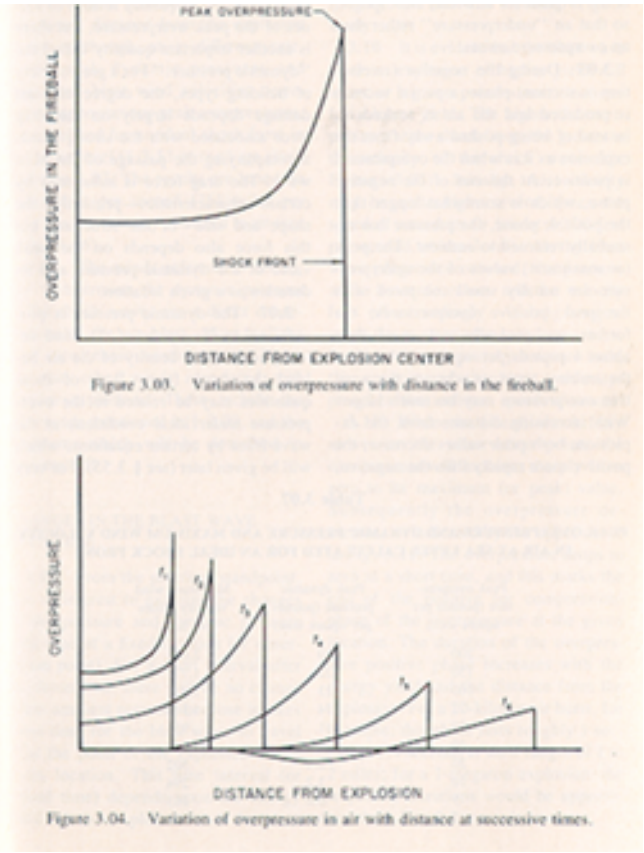


Fig. 4. Shape of the shock pressure wave with time. Note that as the wave propagates outward, the duration of the positive overpressures increase and eventually a rarified region forms behind. From Glasstone and Dolan, p. 81.

An interesting intensification occurs, however when the blast wave reflects from the ground. The reflected blast wave, as shown in Figure 5, then travels through air which

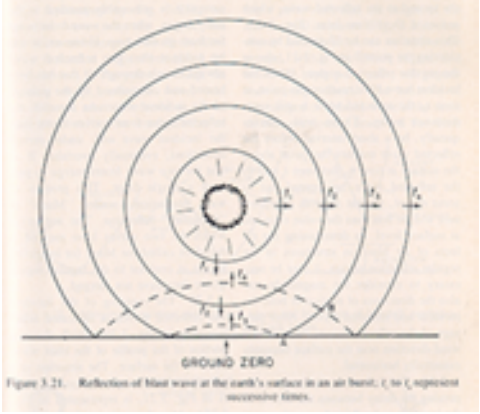


Fig. 5. Formation of the regular reflection region. From Glasstone and Dolan, p. 87.

has a higher temperature and corresponding acoustic velocity than the ambient air because it has already been shocked. This allows the reflected wave to catch up to and reinforce the initial blast wave, increasing the overpressures near the surface in what is called the Mach Front, shown schematically in Figure 6 and pictorially in Figure 7.

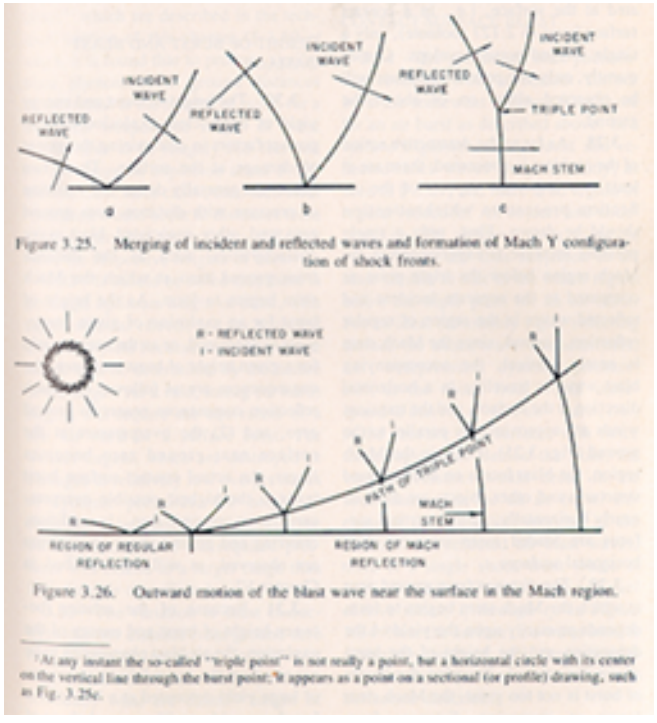


Fig. 6. The formation of the Mach stem. From Glasstone and Dolan, p. 89.

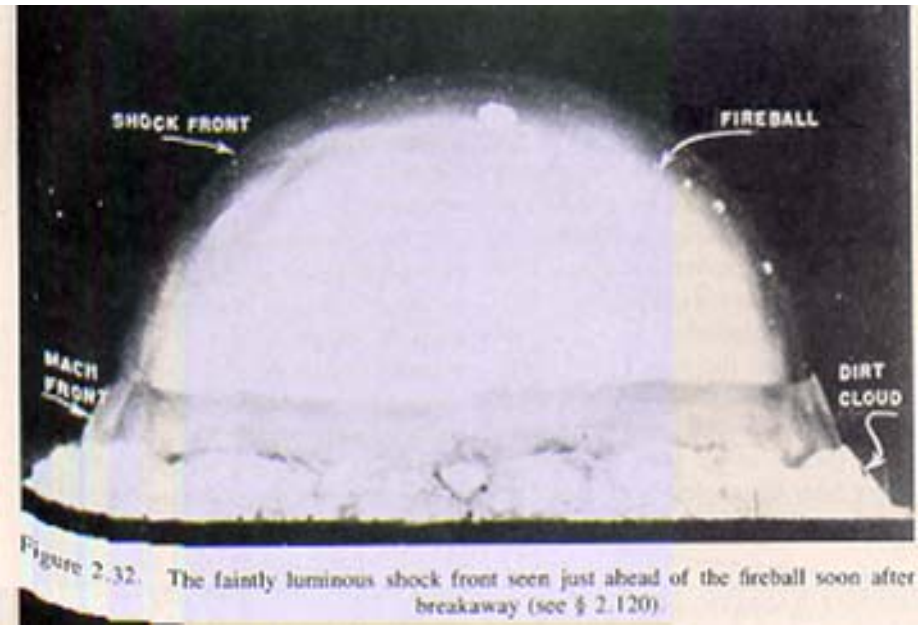


Fig. 7. Picture of fireball shortly after hydrodynamic separation. Note the faintly visible glow from the shock wave and the Mach front. From Glasstone and Dolan, p. 39.

The characteristics of the single shock front are uniquely related by the Rankine-Hugoniot equations (see 3.55 of Glasstone and Dolan, 1977). A table of the peak overpressures and associated velocities and dynamic pressure (kinetic energy of the flow) are given in Figure 8. It should be mentioned that as the blast wave propagates outward, a rarification of as much as 4 psi below normal atmospheric pressure (14.7 psi) can occur behind the initial positive phase, leading to sudden cloud formation, as in a Wilson chamber. These clouds are hence called Wilson clouds and can be seen in Figure 9 as a series of halos where the rarified region of the blast wave intersects with moist layers. As the shock travels upward, it encounters decreasing density and can sharpen into an audible acoustic wave with very fast rise times. This shock can be reflected downward to the ground several hundred kilometers away by a temperature inversion or high winds aloft, causing distant damage. Once the pressure in the fireball region drops to the

ambient pressure, it can do no more work laterally, but the stage is set for hydrostatic adjustment to occur.

**Table 3.07**

**PEAK OVERPRESSURE AND DYNAMIC PRESSURE AND MAXIMUM WIND VELOCITY IN AIR AT SEA LEVEL CALCULATED FOR AN IDEAL SHOCK FRONT**

| Peak overpressure (pounds per square inch) | Peak dynamic pressure (pounds per square inch) | Maximum wind velocity (miles per hour) |
|---|---|---|
| 200 | 330 | 2,078 |
| 150 | 222 | 1,777 |
| 100 | 123 | 1,415 |
| 72 | 74 | 1,168 |
| 50 | 41 | 934 |
| 30 | 17 | 669 |
| 20 | 8.1 | 502 |
| 10 | 2.2 | 294 |
| 5 | 0.6 | 163 |
| 2 | 0.1 | 70 |

Fig. 8. Table of peak overpressures and corresponding maximum wind velocities that are developed. For a one Mt burst at a range of one mile, peak overpressures are 45 psi. For a range of two miles, overpressures drop to 17 psi. At five miles, overpressures of a little less than 4 psi are observed. The minimal damage threshold of 2 psi is observed at a range of 8 miles. From Glasstone and Dolan, p. 82.

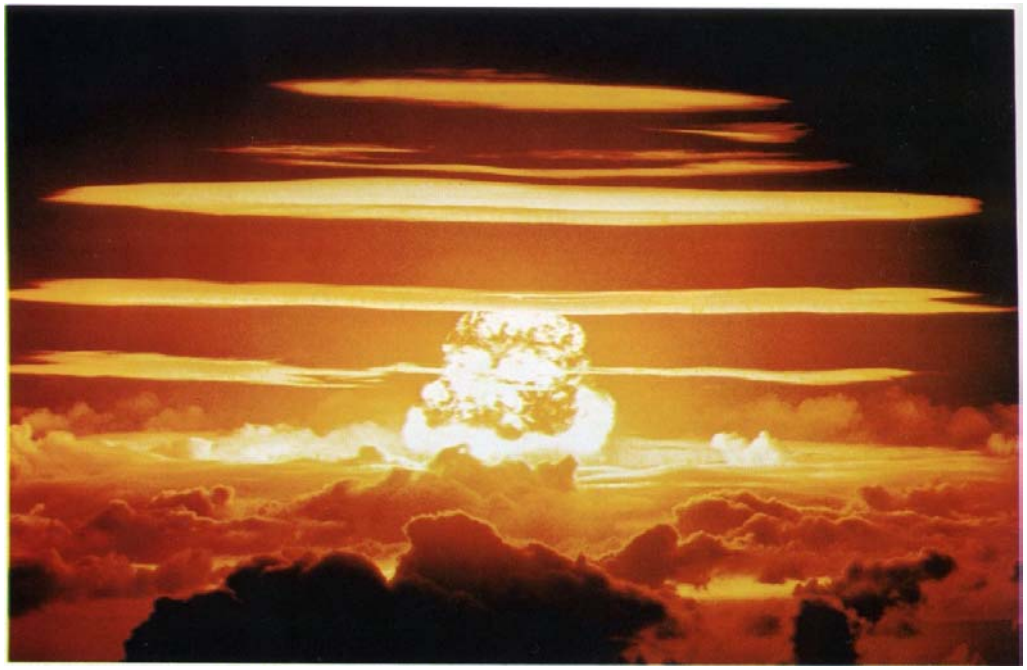

Fig. 9. Photo of the June 25, 1956 Redwing Dakota shot (1.1 Mt yield) off Bikini Atoll. Wilson cloud formation can be seen in the rarified region of the behind the shock wave. The haloes are formed due to the spherical geometry of the shock wave intersecting with moist layers of the ambient atmosphere. The fireball region is visible at the center. Taken from http://fas.org/nuke/hew/Usa/Tests/Redwing.html.

**4. Hydrostatic (and Geostrophic) Adjustment**

Hydrostatic balance, or mechanical balance, is between the vertical pressure gradient and gravity forces. When the atmosphere is disturbed away from mechanical equilibrium, it adjusts back to a balanced state via the process of hydrostatic adjustment, during which bulk movements occur, exciting gravity-acoustic waves that radiate away. A general theory of hydrostatic adjustment is presented by Kalashnik (1999). Basically, the final state, in which total energy is minimized, is determined completely by the initial state and can be found using variational methods similar to those of geostrophic adjustment theory (in which conservation of potential vorticity allows determination of the final state).

The hydrostatic adjustment process begins within a few seconds of the blast, as the heated air in the fireball region rises. If the size of the fireball region is on the order of the density scale height of the atmosphere (about 4.3 miles), it will rise ballistically, overshooting large amounts of denser air to great heights. If the size is considerably smaller, the rise will be due to buoyant forces.

For a one Mt blast with lapse rates normally found over a continental region in the mid-latitudes, the fireball rises for the first minute at an average of 300 mph, reaching a height of nearly six miles. As the updraft rises, the shear at the top surface of the updraft generates a toroidal circulation as shown in Figure 10 in which cooler outside air is drawn in at the bottom center and mixed with the hotter, less dense air inside. If the blast occurs near the surface, dust is drawn up into the cloud via a stem, giving the familiar ‘mushroom’ cloud as shown in Figure 11.

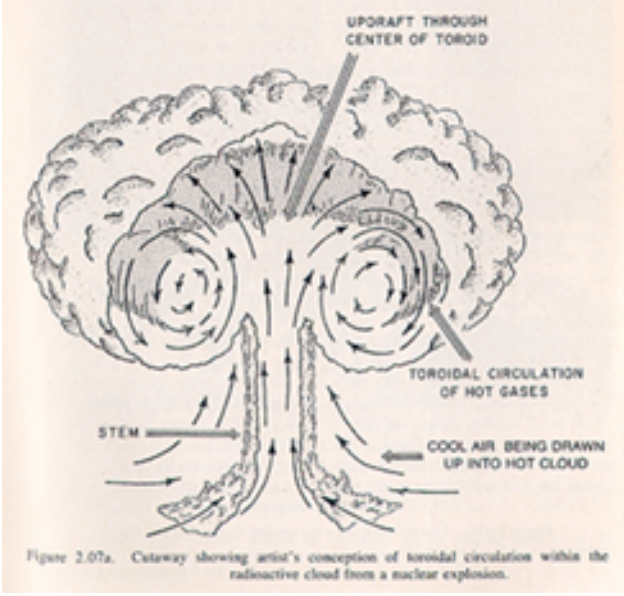


Fig. 10. Due to the shear between the outer edge of the updraft and the surroundings, a toroidal circulation develops, giving the updraft the familiar mushroom shape. From Glasstone and Dolan, p. 29.

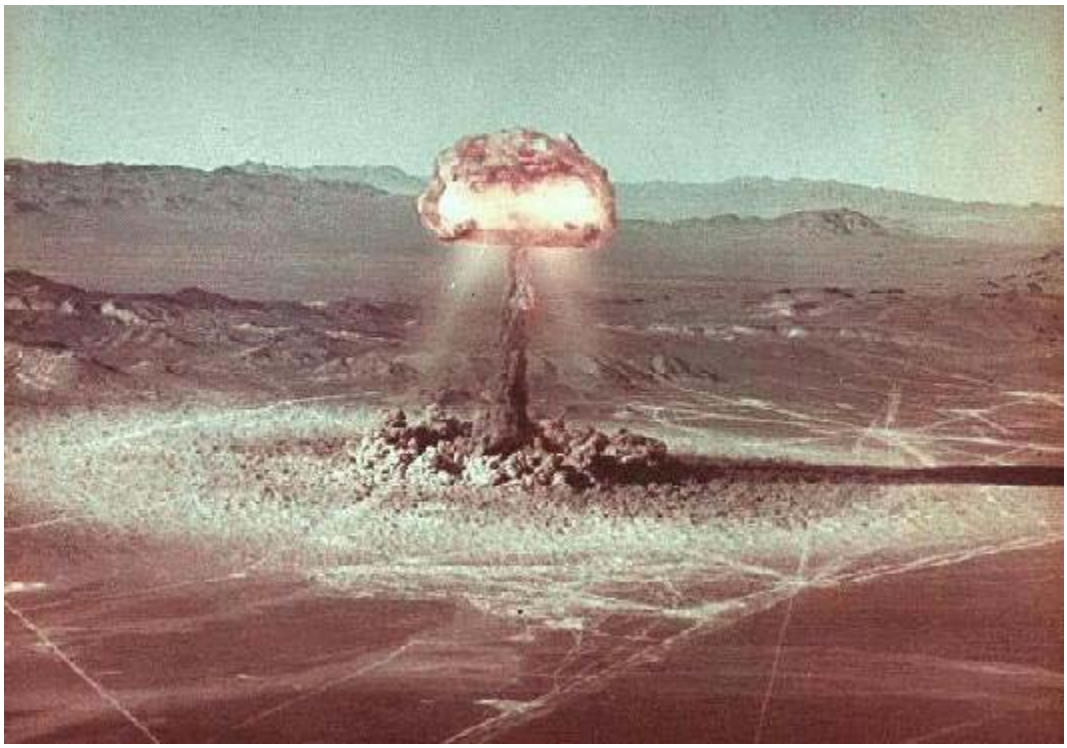

Fig. 11. The early stage mushroom cloud and stem several seconds after detonation. Note the shock effects on the surrounding ground and the formation of a base surge. From 'The Gallery of U. S. Nuclear Tests' web page: http://fas.org/nuke/hew/Usa/Tests/Busterj.html.

The cooler environmental air dilutes the buoyancy of the updraft, slowing its rate of ascent. After two and half minutes, it reaches an altitude of ten miles and is still moving at an upward speed of 140 mph. The rapid cooling with height causes moisture to condense, releasing latent heat which helps to sustain the updraft. Above the tropopause, strong static stability slows the rising 'bubble' and forces it to spread out. After three and half minutes, the bubble is at a height of twelve miles and only rising at 27 mph. Again it takes on the appearance of a gigantic, white mushroom cloud, as shown in Figure 12.

Fig. 12. Photo showing late stage mushroom cloud of Ivy Mike test, Oct. 31, 1952, 10.4 Mt yield. "The mushroom cloud climbed to 57,000 feet in only 90 seconds, entering the stratosphere. One minute later it reached 108,000 feet, eventually stabilizing at a ceiling of 120,000 feet. Half an hour after the test the mushroom stretched 60 miles across, with the base of the mushroom head joining the stem at 45,000 feet. " Taken from 'Gallery of U.S. Nuclear Tests' web page: http://fas.org/nuke/hew/Usa/Tests/Ivy.html.

As the mushroom cloud rises and penetrates the stratosphere, waves are generated. "Since the propagation of these waves is controlled by both the

compressibility of the air and gravitational effect, they are called acoustic-gravity waves" (from Tahira, 1982). For the large explosions we are considering, the gravitational effect is more important and the waves are closer to regular gravity waves[4]. Their generation is virtually the same as for an intense thunderstorm penetrating the stratosphere (Gedzelman, 1983) and is shown in Figure 13. Pfeffer and Zarichny (1962) investigated the phase and group velocities of the various acoustic and gravity modes of the waves and found that "they show normal dispersion in the range of periods from one to ten minutes and inverse dispersion at shorter periods." A sensitive microbarograph can record the resulting wave train thousands of kilometers from the blast. An example of such a trace is shown in Figure 14.

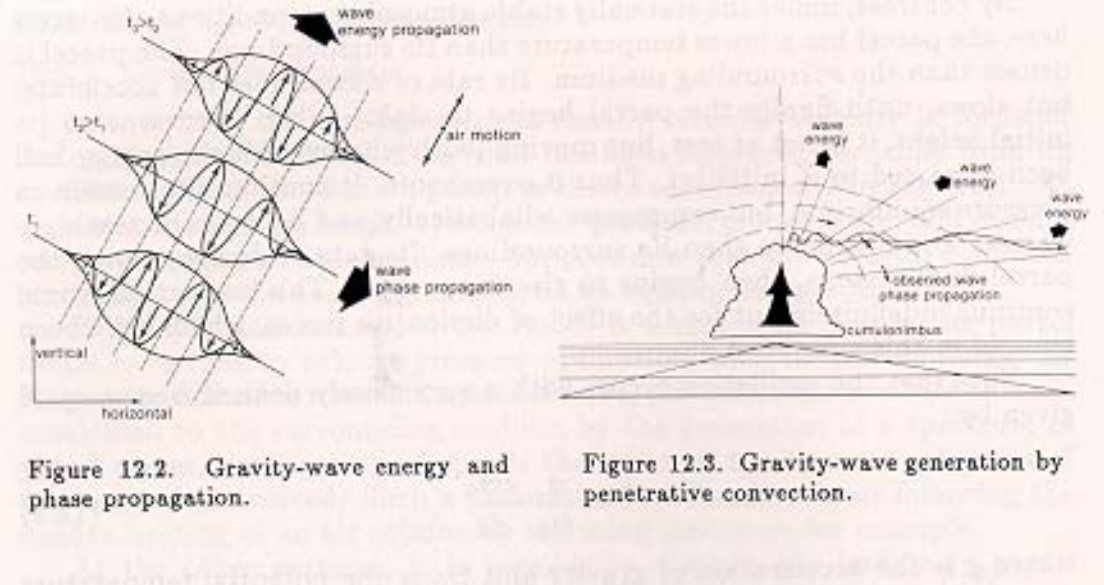


Figure 12.2. Gravity-wave energy and phase propagation.

Figure 12.3. Gravity-wave generation by penetrative convection.

Fig. 13. Generation and propagation characteristics of gravity-acoustic waves due to deep penetrative convection. Note that the waver energy radiated in the more horizontal directions is of longer periods than the vertically propagating wave energy. From Hooke (1986).

[4] Smaller explosions generate waves with higher frequencies, known as infrasound. These waves have propagation characteristics more in keeping with acoustic waves – in which gravity is irrelevant and reflection and refraction depend more on the how the local speed of sound varies along the ray path.

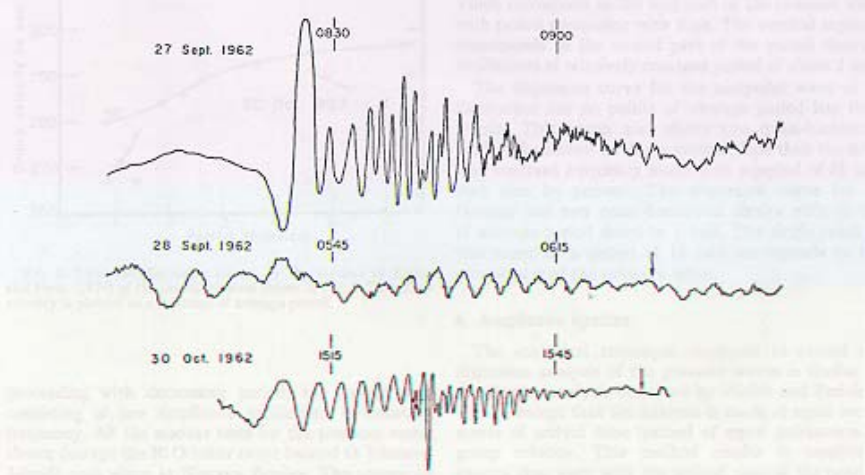


FIG. 1. Pressure waves recorded at Socorro from atmospheric nuclear tests on 27 September and 30 October 1962. The 28 September trace is an antipodal wave of the 27 September test.

Fig. 14. Pressure waves recorded at Socorro from nuclear tests. The Oct. 30, 1962 trace corresponds to the Dominic Housatonic test, an 8.3 Mt airburst near Johnston Atoll (Simon and Robinson, 1997). Figure taken from McCrory (1967).

For megaton scale explosions, another interesting phenomenon occurs with the upward traveling gravity-acoustic waves. As the wave energy propagates upward, it encounters the rapidly decreasing density of the atmosphere. The wave energy is concentrated on ever decreasing mass, so the amplitude of the motions becomes very large. After about thirteen minutes, the waves reach the ionosphere at an altitude of 250 km. Although the upward propagating modes are of short wavelength, they arrive in a horizontal plane first at the point directly above the plane, then in an expanding circle around this point, whose radius is determined by the distance from the blast and propagation speed. Very long period gravity waves are thus excited in a horizontal region several hundred kilometers across, with vertical amplitude motions of 6-8 km and group velocities of about 750 meters per second (Herron, 1971).

In the mid-latitudes, the ratio of the initial heating (which we take to be on the order of tens of kilometers) to the Rossby radius of deformation is quite small, and in

addition, the heating is very rapid, so geostrophic adjustment theory predicts that little balanced flow should remain, with nearly all the energy being radiated away as gravity waves (or in this case, acoustic-gravity waves)[5].

**5. Tertiary Effects**

Tertiary effects may linger after most of the energy has been dispersed to hundreds or thousands of kilometers away. The large amount of thermal energy released into the surroundings may ignite large forest areas, leading to firestorms and other after affects. Dust kicked into the air may alter regional cloud properties. The local boundary layer may take quite some time to return back to a normal state in sync with the diurnal heating cycle. In general, most of these tertiary effects are in keeping with general mesoscale dynamics. Synoptic circulations, turbulent mixing, and diffusion will eventually smear out any residual heat and aerosol anomalies, leading to a post-blast state that is indistinguishable from the pre-blast state within a time frame of several hours to several days. The acoustic-gravity waves that have propagated far from the blast location may trigger or suppress convective activity, but they weaken as they degrade to heat and after traversing the globe several times, they too are indistinguishable from the everyday 'noise' of the atmosphere. The final state atmosphere is just a tad warmer than it was before, and this excess energy radiates out to space, maximizing the entropy.

[5] An interesting exception may occur if the blast happens in the center of a strong hurricane in which the local Rossby radius, which depends on inversely on vorticity, is also on the order of tens of kilometers. Then a significant portion of the heating may be converted into balanced flow.

**5. Conclusion and Summary**

The atmosphere adjusts back to a 'normal' state following an extremely large explosive event by several mechanisms acting over widely varied time and spatial scales. First an initial phase rapidly distributes the energy by radiative means to a volume of air equal to several cubic kilometers within a few milliseconds. This sets the stage for a second phase of hydrodynamical expansion over several minutes that further distributes the energy over tens of cubic kilometers by means of a strong pressure wave. The heated air that remains after the first and second phases is then distributed vertically by a third phase of hydrostatic adjustment in which the mechanical equilibrium is attained via the radiation of acoustic-gravity waves over a time period of several seconds to about fifteen minutes. As the acoustic-gravity waves from the various adjustment processes are dissipated globally and remaining local heat is mixed by diffusion and normal mesoscale processes, the atmosphere returns to a balanced state indistinguishable from the initial state before the explosion. This final state is one in which the total system energy has been minimized and the total entropy are maximized. In essence, nearly all the energy of the explosion degrades to heat in the global atmosphere and is lost to space.

## REFERENCES

Gedzelman, S. D., 1983: Short-Period Atmospheric Gravity Waves: A Study of Their Statistical Properties and Source Mechanisms. *Mon. Wea. Rev.,* **111**, 1293-1299.

Glasstone, S., Dolan, P. J., 1977: The Effects of Nuclear Weapons, 3rd Ed. Department of Defense, Department of Energy.

Heron, T. J., 1971: Group Velocities of Atmospheric Gravity Waves. *J. Atmos. Sci.,* **28**, 598-603.

Hooke, W.H., 1986: Mesoscale Meteorology, Ed. Peter S. Ray. Amer. Met. Soc.

Kalashnik, M. M., 2000: Hydrostatic Adjustment Theory. *Izvestiya, Atmos. and Oceanic Physics, vol.* **36,** no. 2, 203-209.

McCrory, R. A., 1967: Atmospheric Pressure Waves from Nuclear Explosions. *J. Atmos. Sci.*, **19**, 443-447.

Pfeffer, R. L., Zarichny, J., 1962: Acoustic-Gravity Wave Propagation in the Earth's Atmosphere. *J. Atmos. Sci.,* **19**, 256-263.

Reed, J. W., 1987: Air Pressure Waves from Mount St. Helens Eruptions. *J. Geophys. Res.*, vol. **92**, no. D10, 11,979-11,992.

Simon, S. L., Robison, W. L., 1997: A Compilation of Nuclear Weapons Test Detonation Data for U.S. Pacific Ocean Tests. *Health Physics*, vol. **73**, no. 1, 258-264.

Tahira, Makoto, 1982: A Study of the Infrasonic Wave in the Atmosphere. II. Infrasonic Waves Generated by the Explosions of the Volcano Sakura-Jima. *J. Met. Soc. Japan*, vol. **60**, no. 3, 896-907.

Taylor, Sir G., 1950: The Formation of a Blast Wave by a Very Intense Explosion. I. Theoretical Discussion. *Proc. Roy. Soc. A,* ***201***, 159-174.

Taylor, Sir G., 1950: The Formation of a Blast Wave by a Very Intense Explosion. II. The Atomic Explosion of 1945. *Proc. Roy. Soc. A,* ***201***, 175-186.

von Neumann, J., 1947: The Point Source Solution. *Blast Wave*, ch. 2. Los Alamos Sci. Lab. Tech. Series, Vol. VII, Pt. II ed. By H. Bethe Aug. 13, 1947, LA-2000.

Some pictures and graphs are taken from the following web sites:

http://www.fas.org/nuke/hew/Wallpaper.html
http://fas.org/nuke/hew/Usa/Tests/index.html
http://nuketesting.enviroweb.org/nukeffct/index.html
http://www.nv.doe.gov/news&pubs/photos&films/testfilms.htm

Additional references not specifically cited:

Batchelor, G., 1996: Life and Legacy of G. I. Taylor. Cambridge University Press.

Kulichkov, S. N., 1992: Long-Range Propagation of Sound in the Atmosphere, A Review. *Izvestiya, Atmos. and Oceanic Physics,* vol. **28,** no. 4, 253-269.

Whitam, B. 1974: Linear and Nonlinear Waves. John Wiley & Sons, Inc.